





Literature Report

Reporter: Wang Guangying

Date: 2020-10-15



Organelle membrane-specific chemical labeling and dynamic imaging in living cells

Tomonori Tamura ^{1,2}, Alma Fujisawa^{1,2}, Masaki Tsuchiya^{1,2}, Yuying Shen¹, Kohjiro Nagao¹, Shin Kawano^{3,4}, Yasushi Tamura⁵, Toshiya Endo^{3,4}, Masato Umeda ¹ and Itaru Hamachi ^{1,2} 

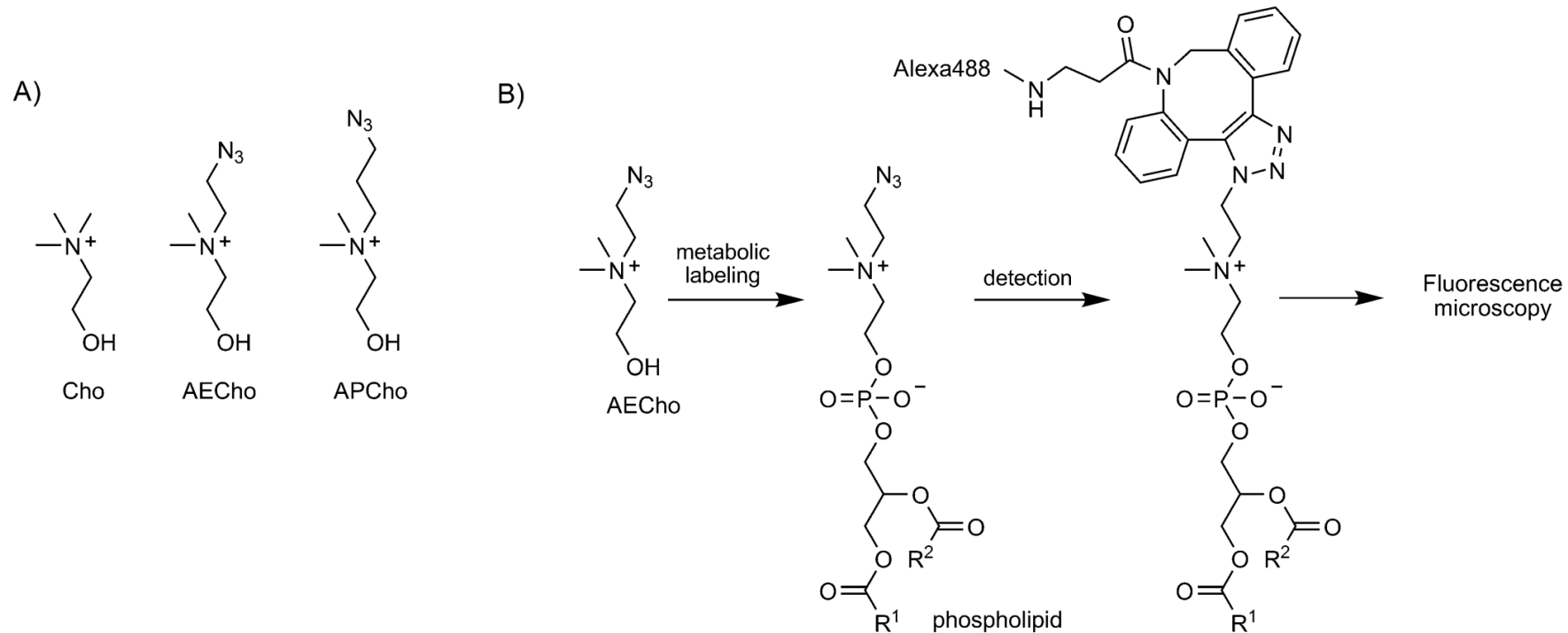
Intracellular Transport of Phosphatidylcholine to the Plasma Membrane

Pulse labeling of CPLs

MIRIAM R. KAPLAN and ROBERT D. SIMONI

Department of Biological Sciences, Stanford University, Stanford, California 94305

J. Cell Biol. **101**, 441–445 (1985)



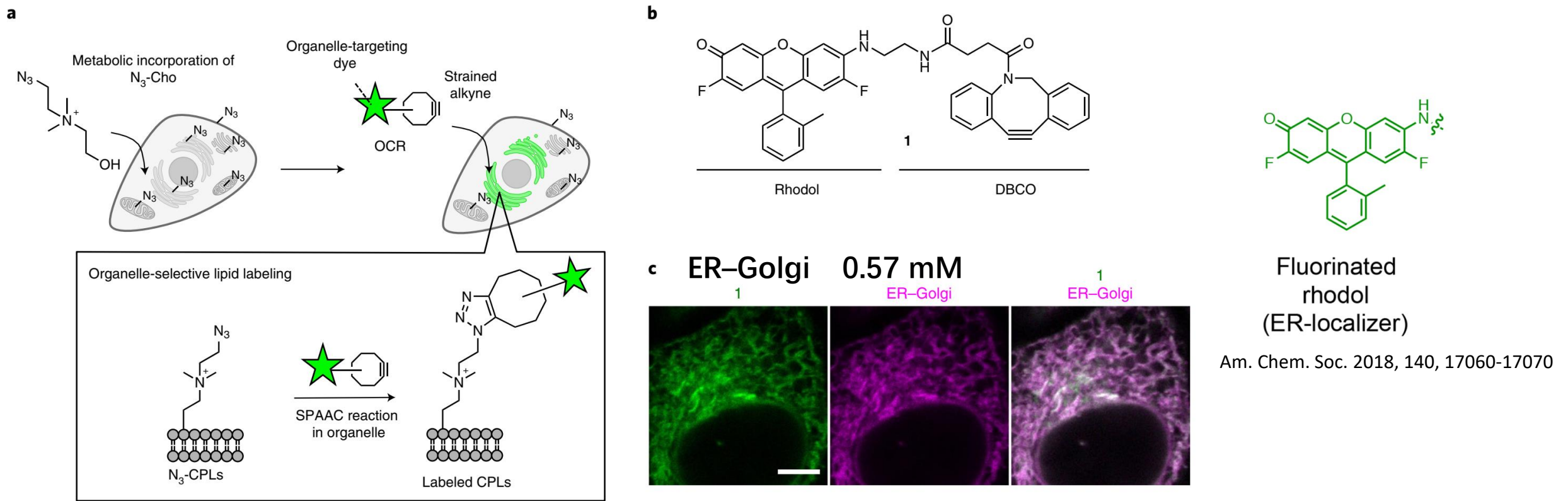
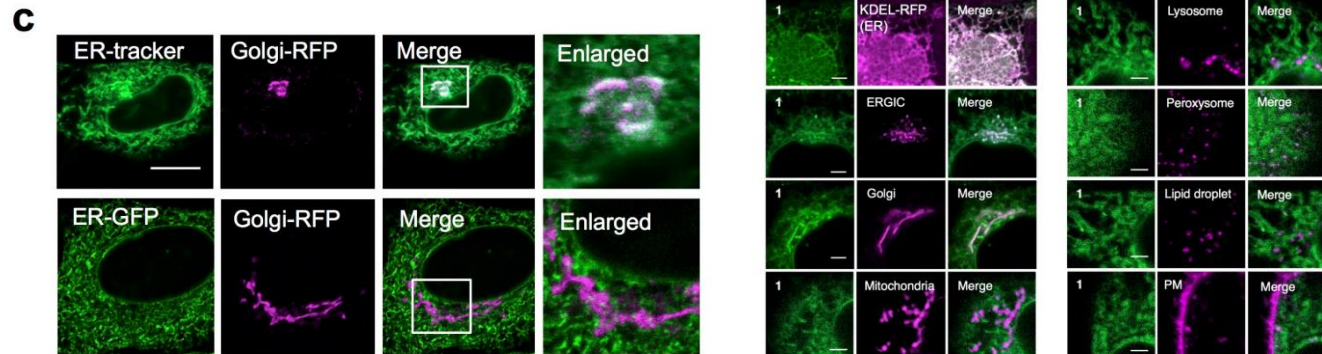


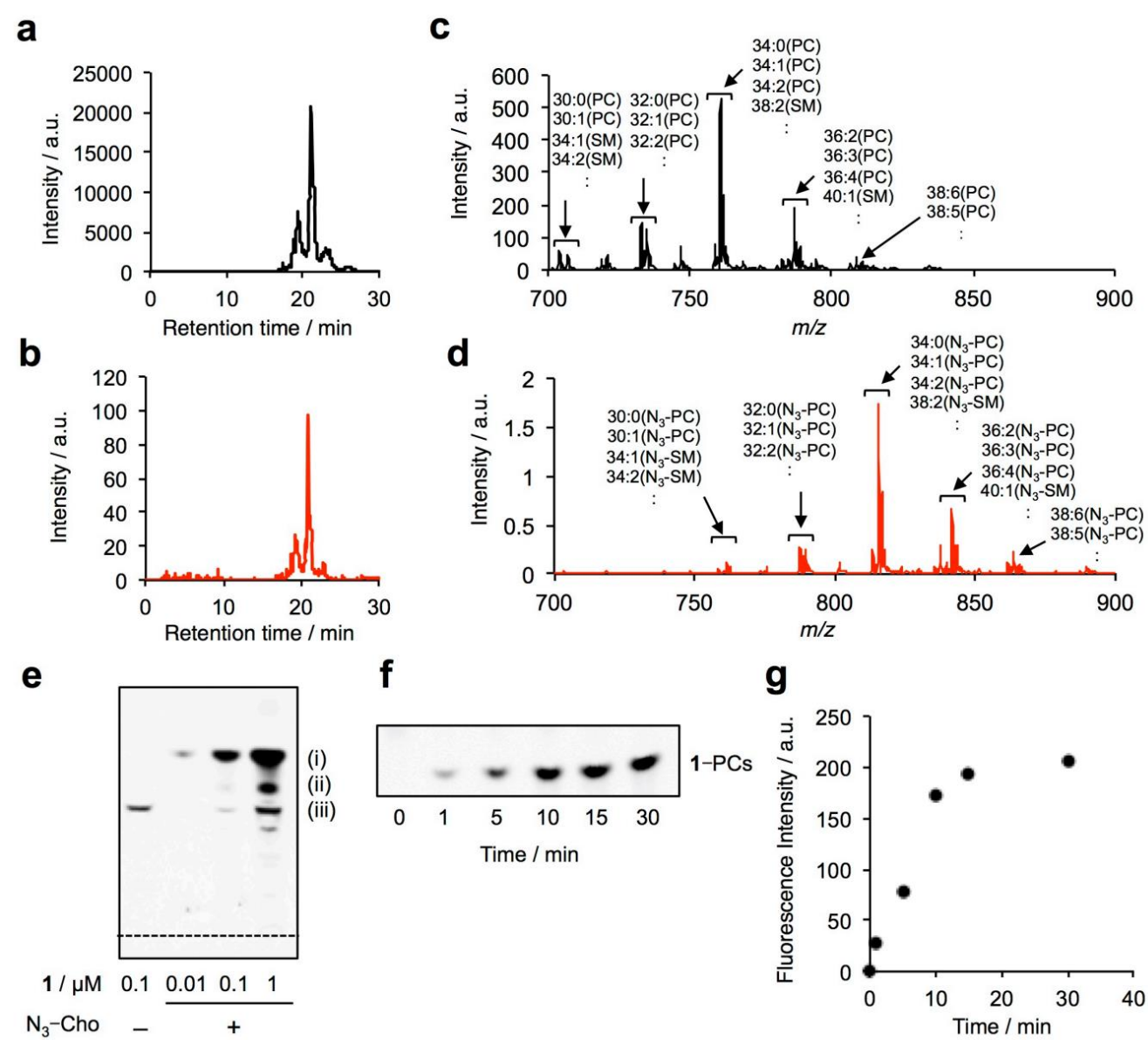
Fig. 1 | ER-golgi-selective PC labeling and imaging in live cells. a, Schematic of organelle-selective lipid labeling with OCR. **b**, Molecular structure of the ER-Golgi OCR **1**. **c**, CLSM images of a HeLa cell treated with **100 nM 1** (green) for 15 min. **ER-Tracker** (magenta) was used for imaging both the ER and Golgi because it stains both in HeLa cells (Supplementary Fig. 1c). Scale bar. 5 μ m

ER-Tracker

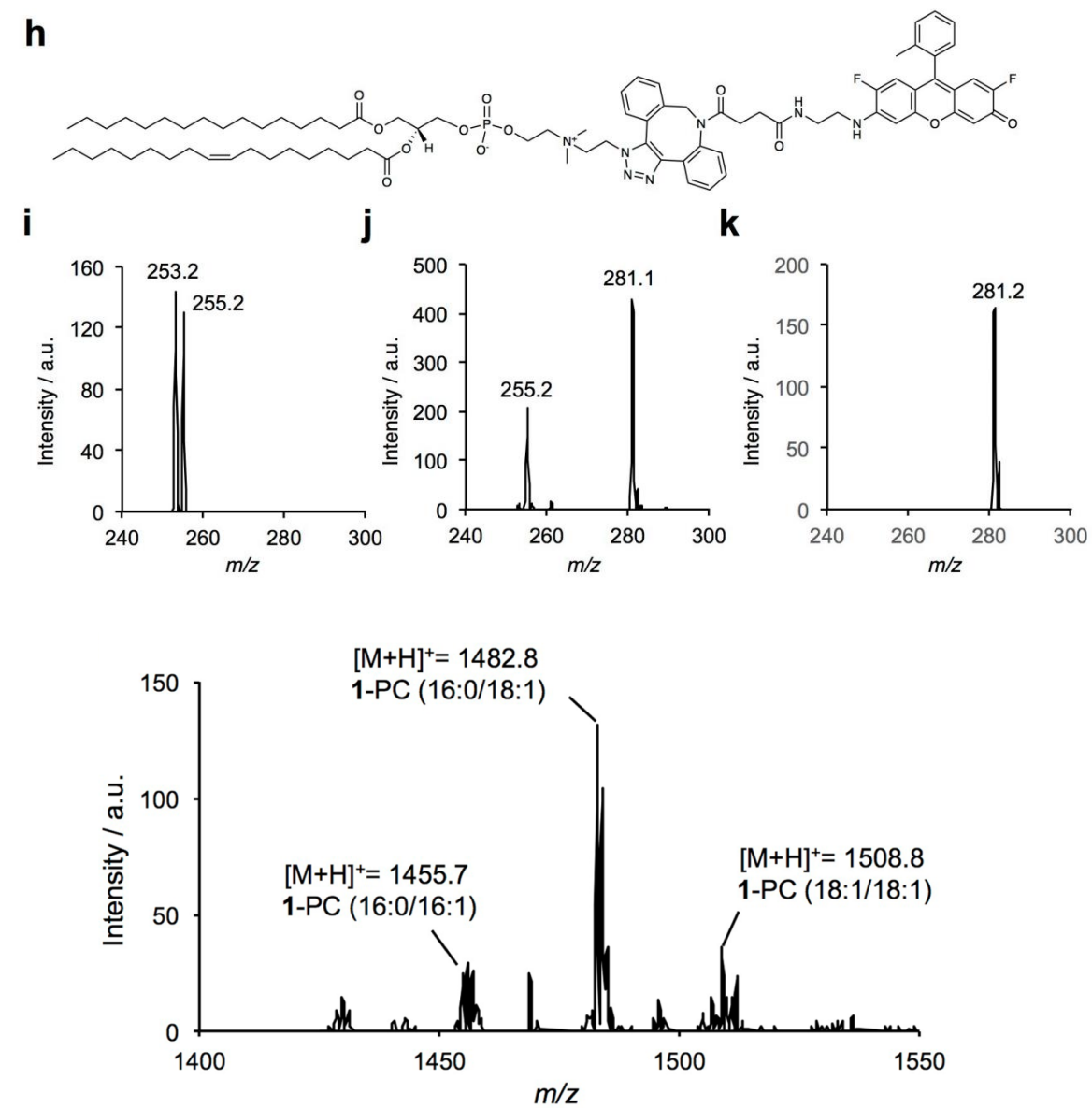


ER, the ER-Golgi, Golgi, mitochondria, lysosomes, peroxisomes, lipid droplets and PMs

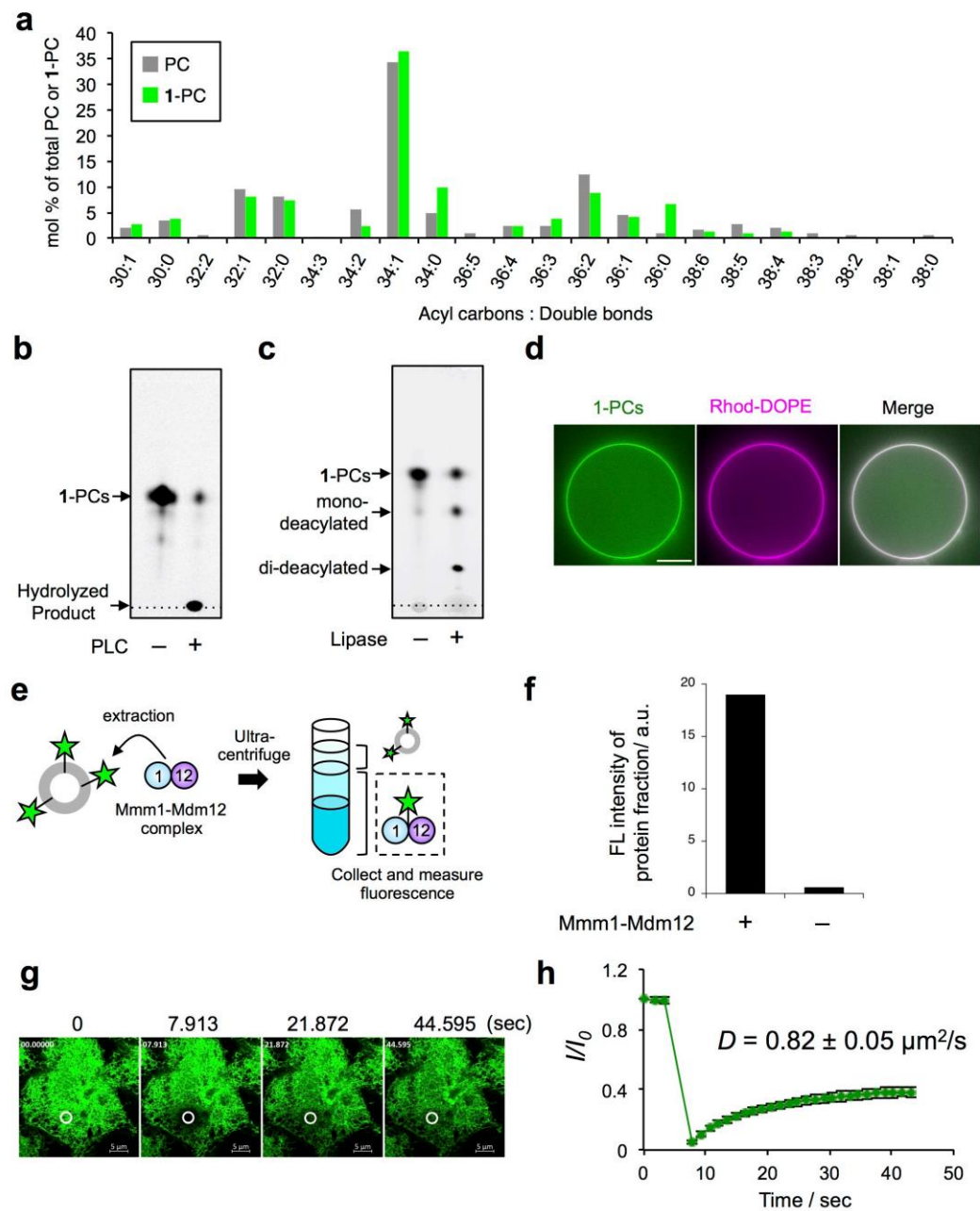
Supplementary Figure 1. Spectroscopic properties and intracellular localization of **1**.



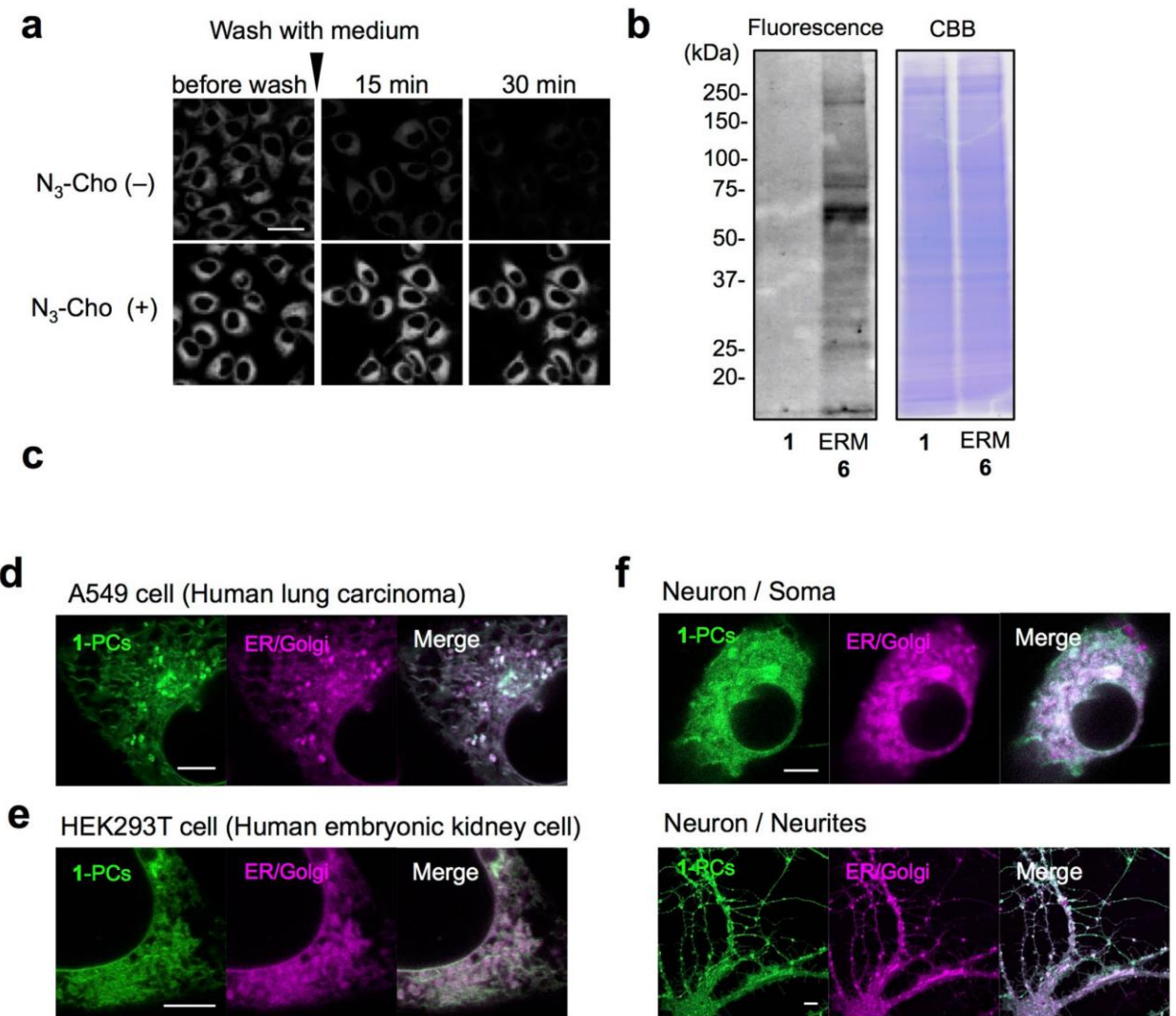
Supplementary Figure 2. LC-MS and TLC analysis of metabolic incorporation of $\text{N}_3\text{-Cho}$ and subsequent spatially limited strain-promoted alkyne-azide cycloaddition (SPAAC) reaction.



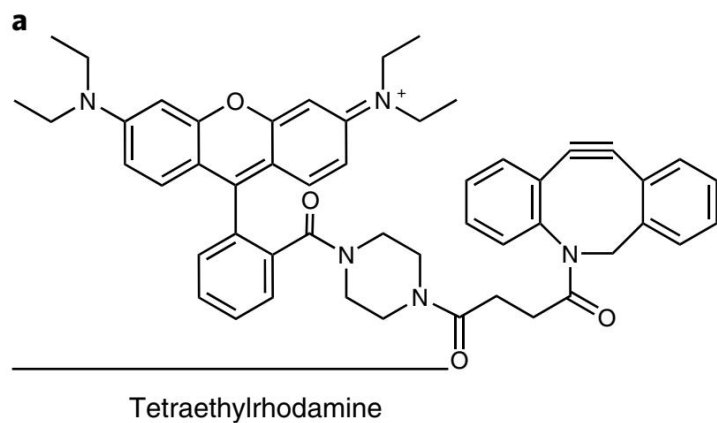
Extended Data Fig. 1 | Product analysis of ER/golgi-selective phosphatidylcholine (PC) labelling in live cells.



Supplementary Figure 3. Biochemical and physical properties of 1-PCs.



Extended Data Fig. 2 | ER/golgi-specific PC labelling with 1



2

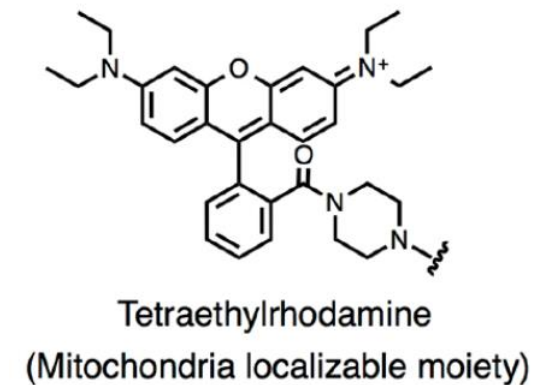
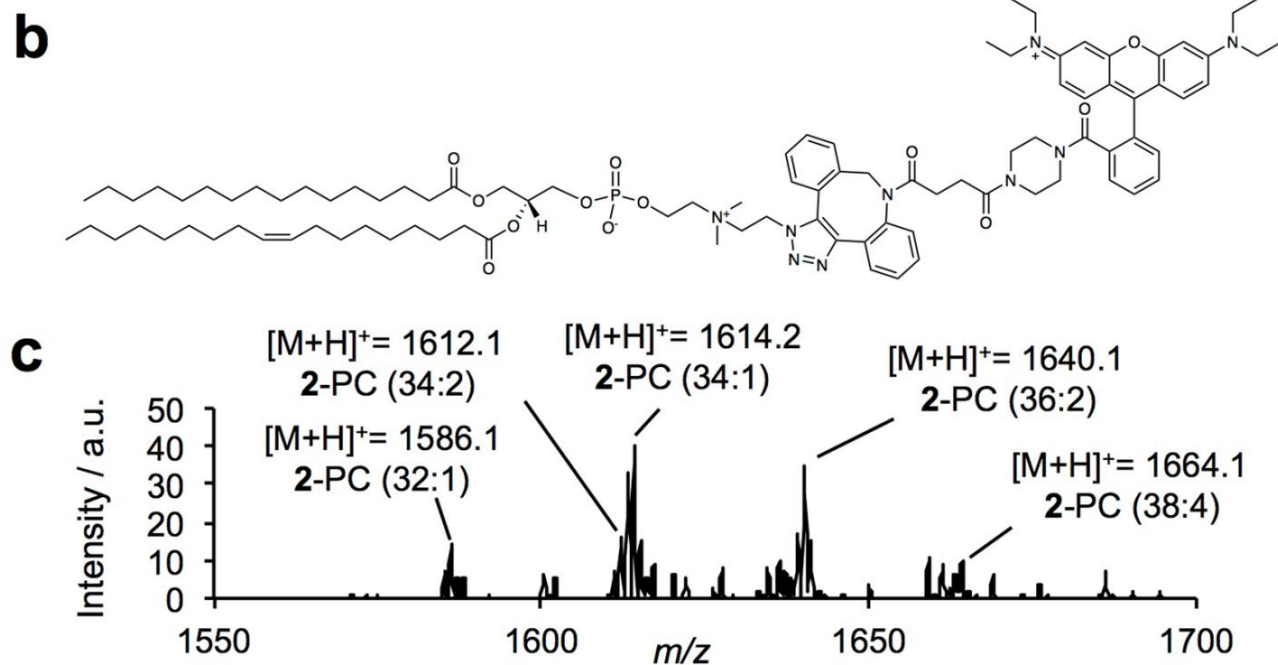
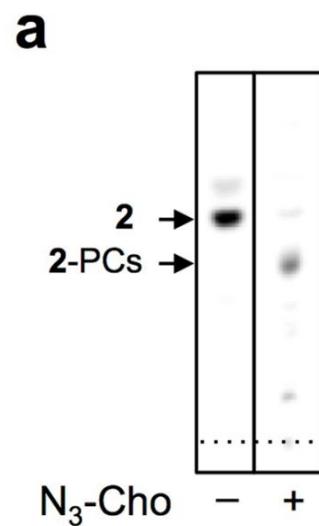


Fig. 2 | Mitochondria-selective PC labeling and imaging

J. Am. Chem. Soc. 2019, 141, 2782-2799



Extended Data Fig. 3 | labelling and imaging of PCs in mitochondria with 2

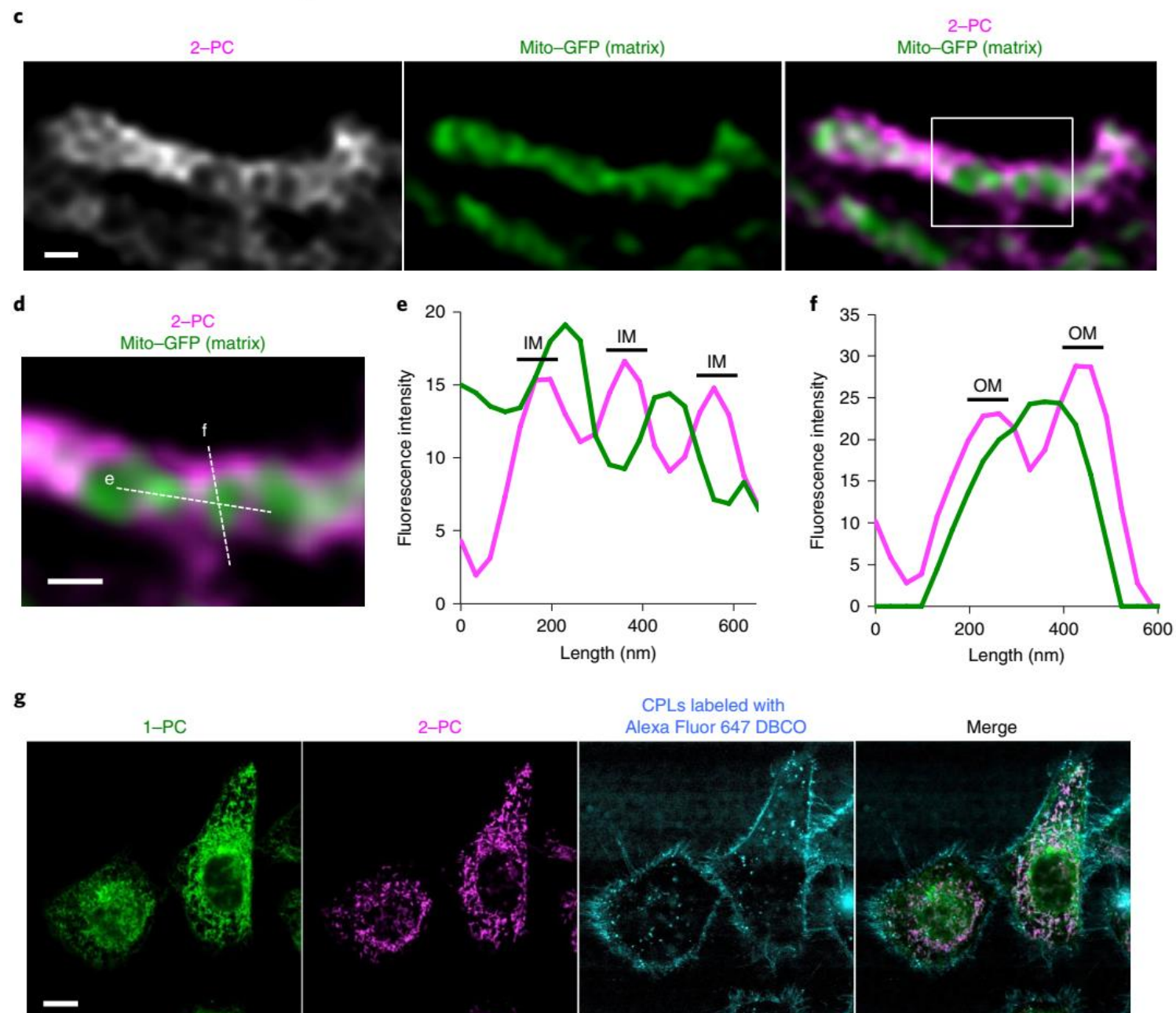
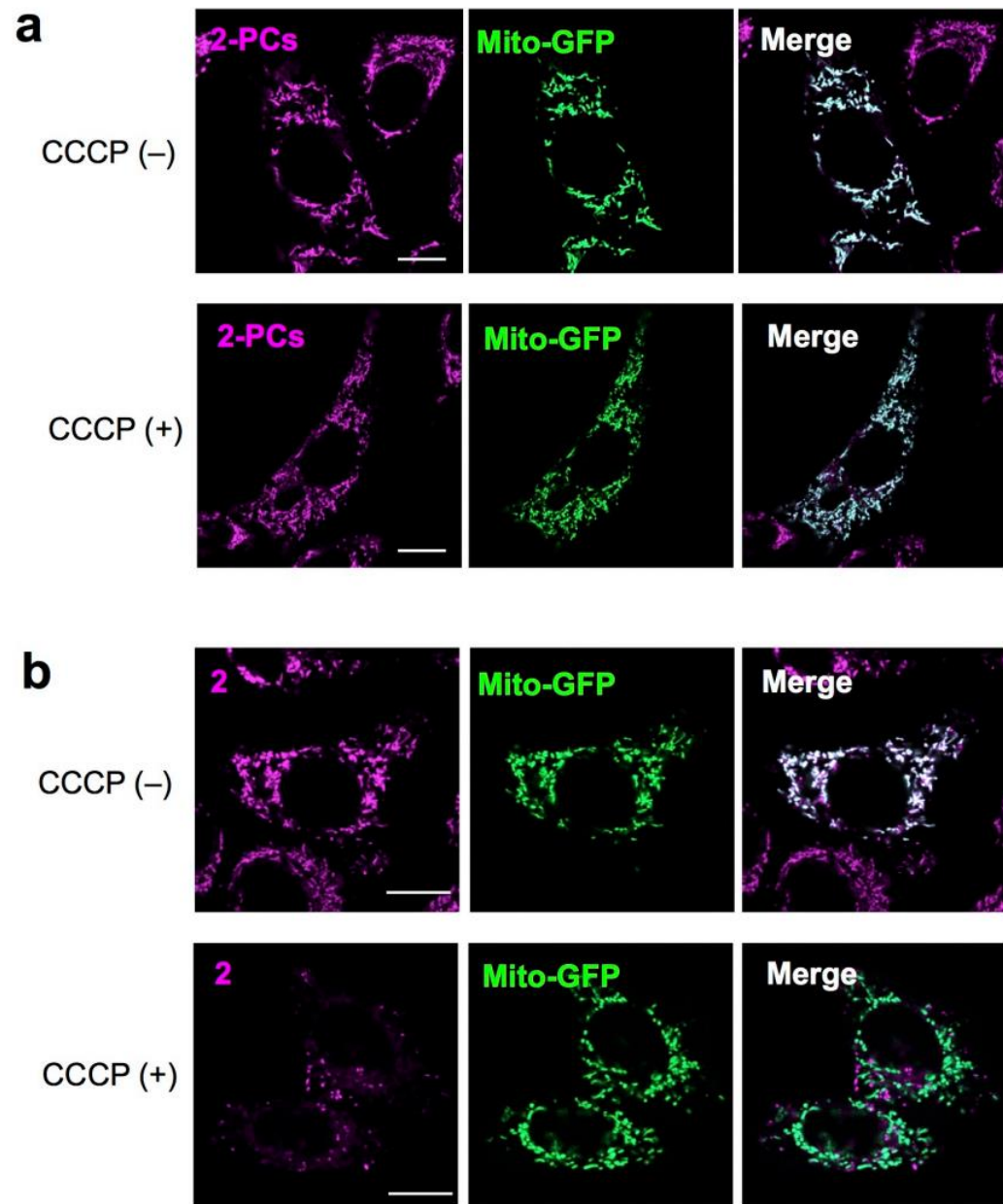
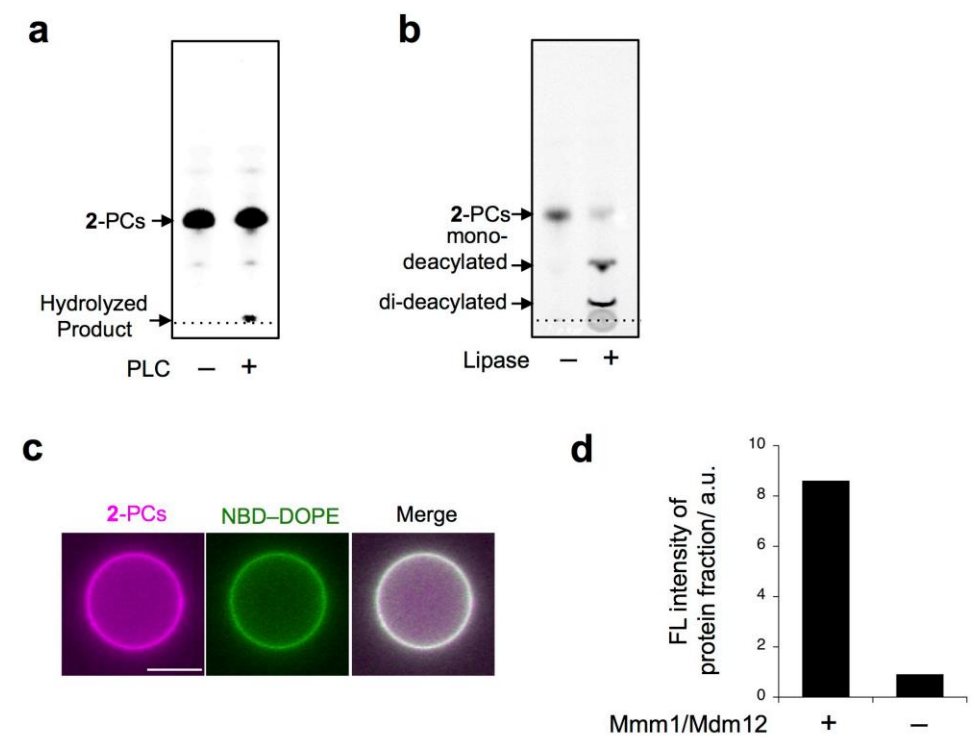


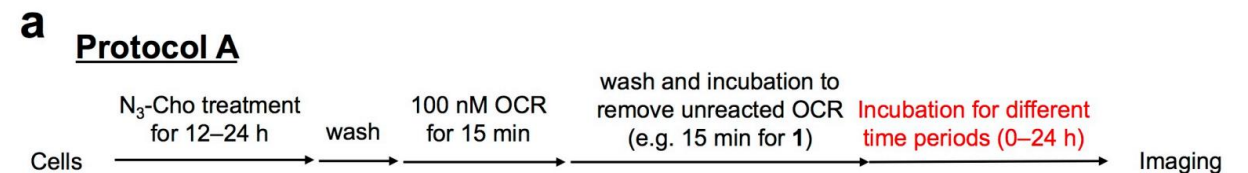
Fig. 2 | Mitochondria-selective PC labeling and imaging



Supplementary Figure 5. Mitochondrial retention of 2-PCs does not depend on the membrane potential.



Supplementary Figure 6. Biochemical and physical properties of 2-PCs.



Supplementary Figure 7. Two different protocols for fluorescent imaging of interorganelle translocation of labelled PCs.

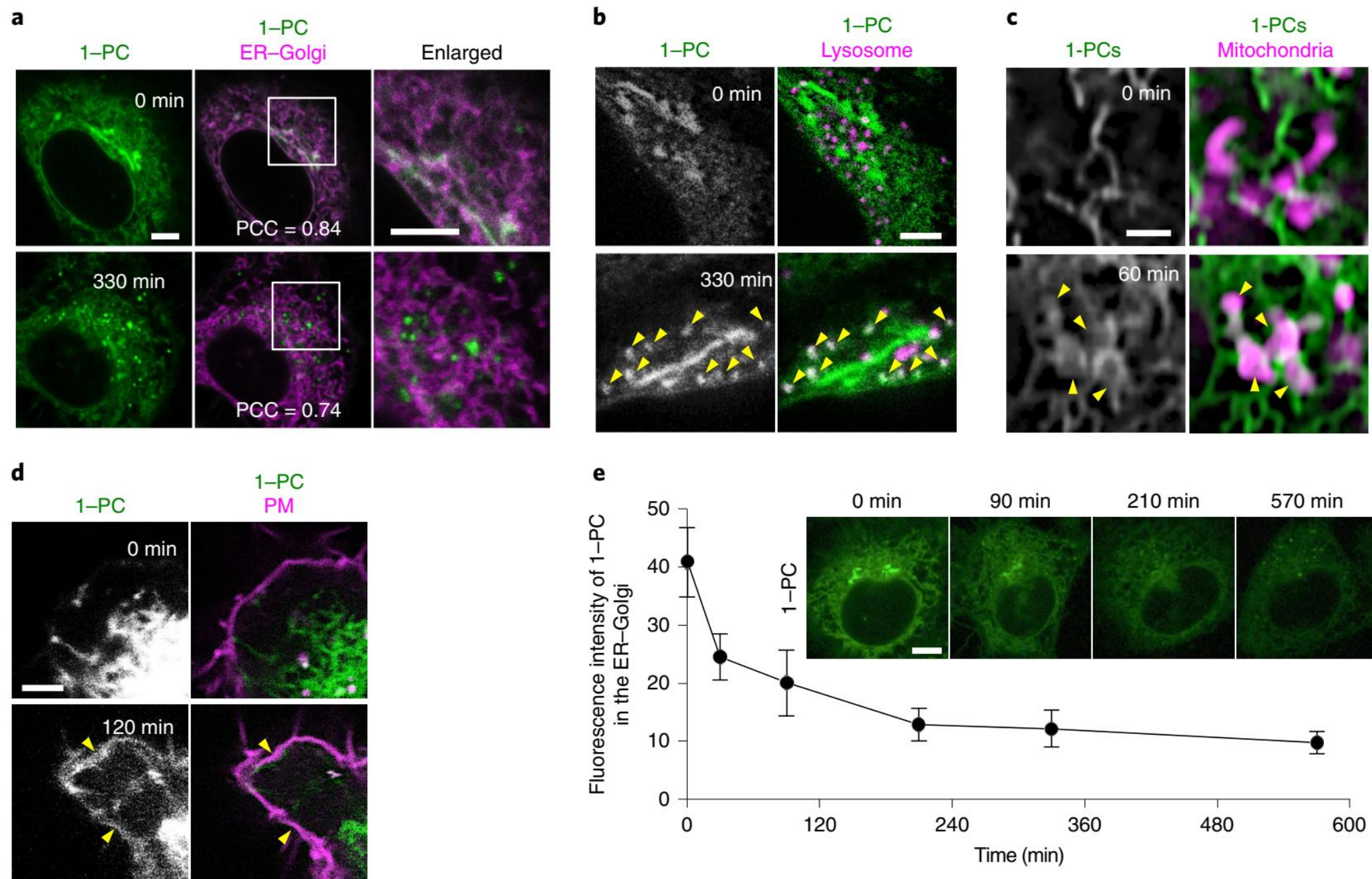
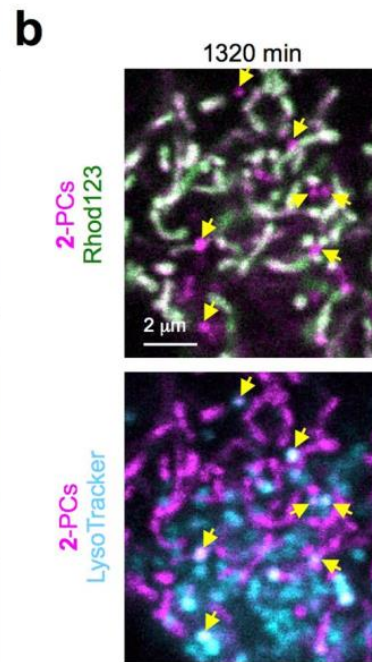
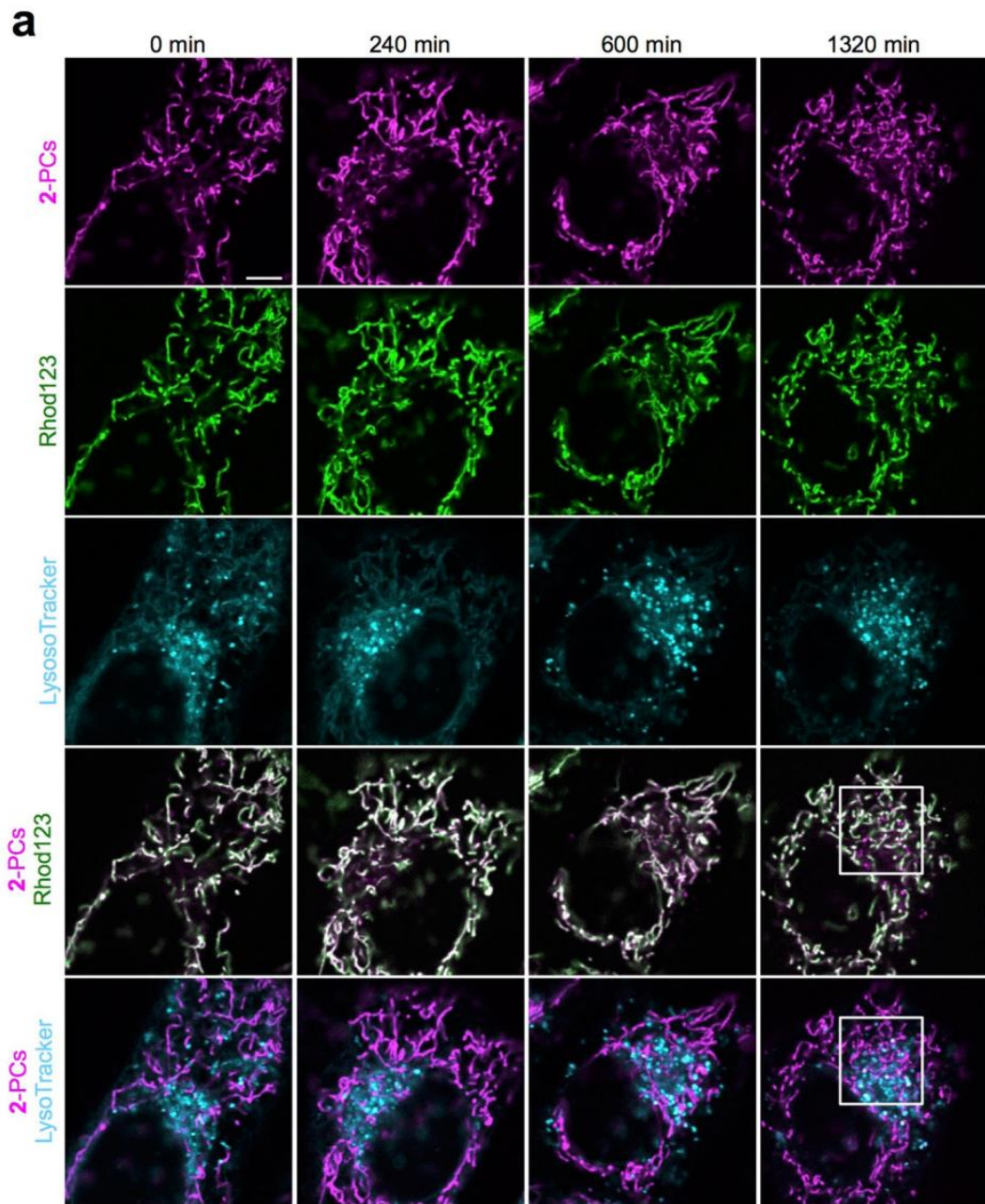
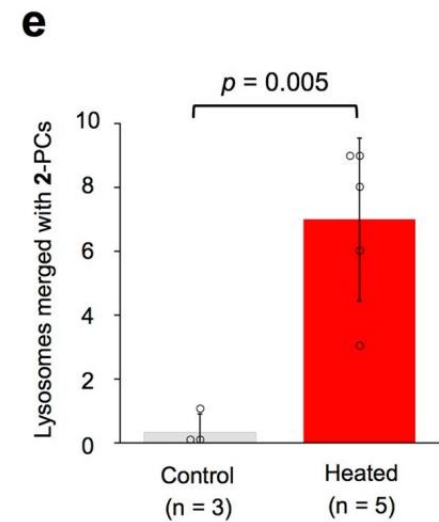
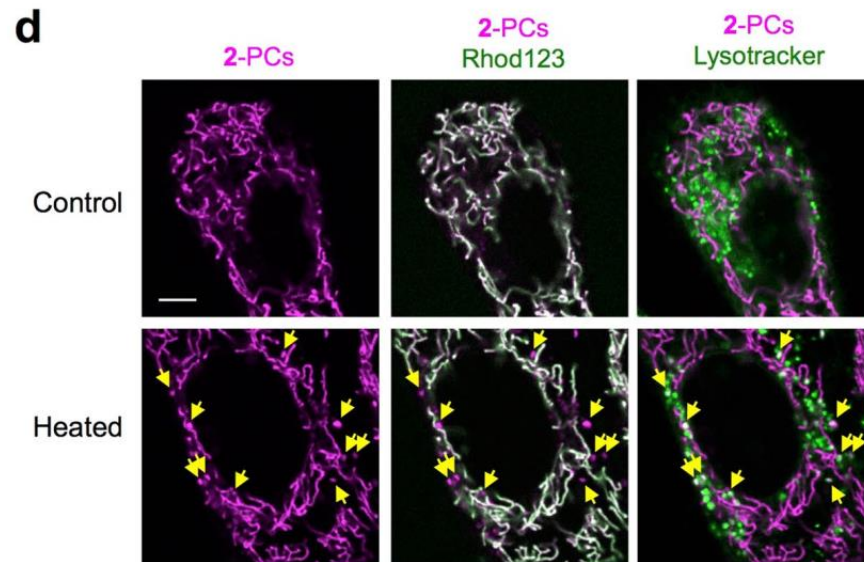
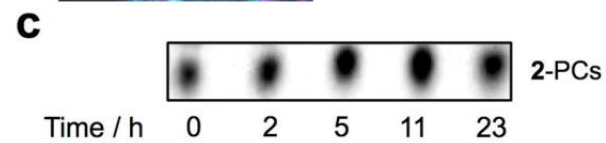
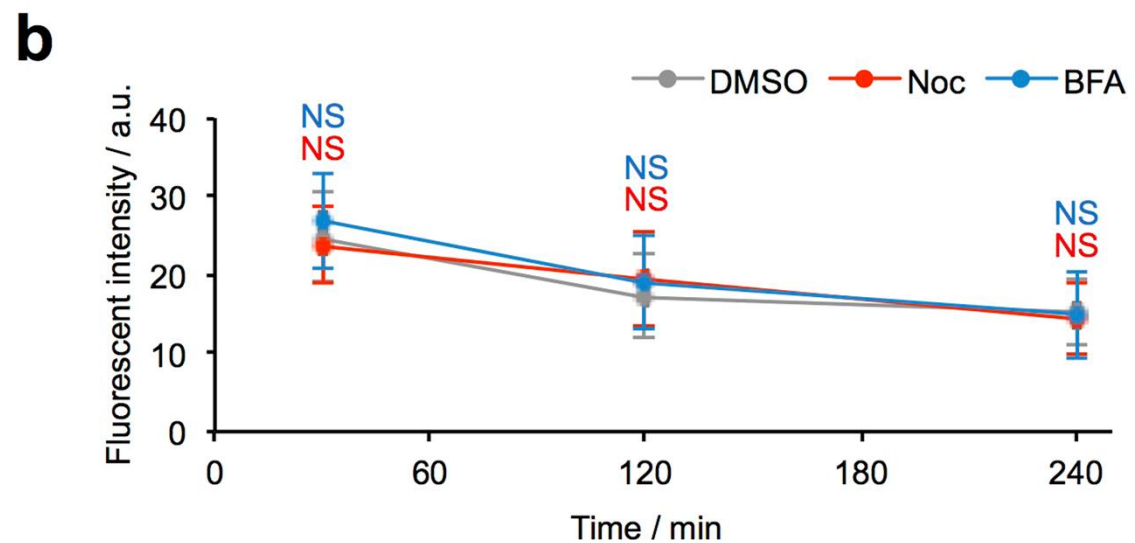
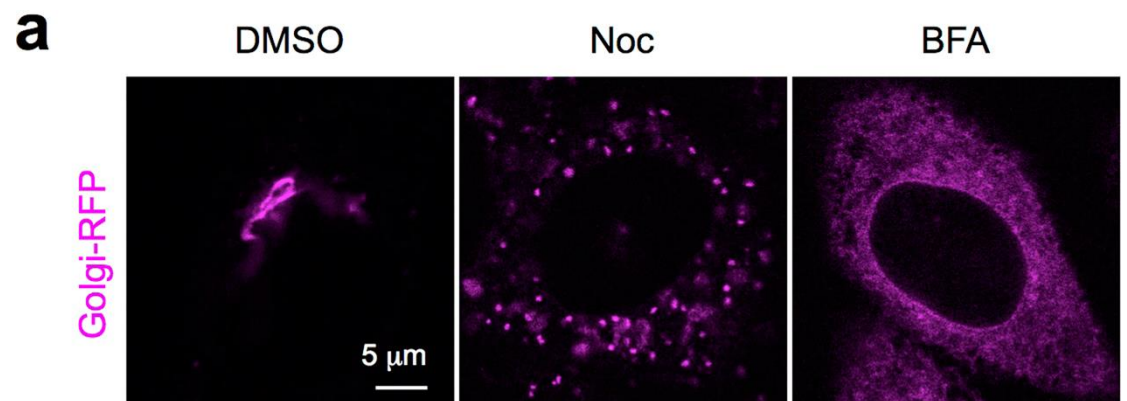


Fig. 3 | live-cell tracing of interorganelle translocation of 1-PC

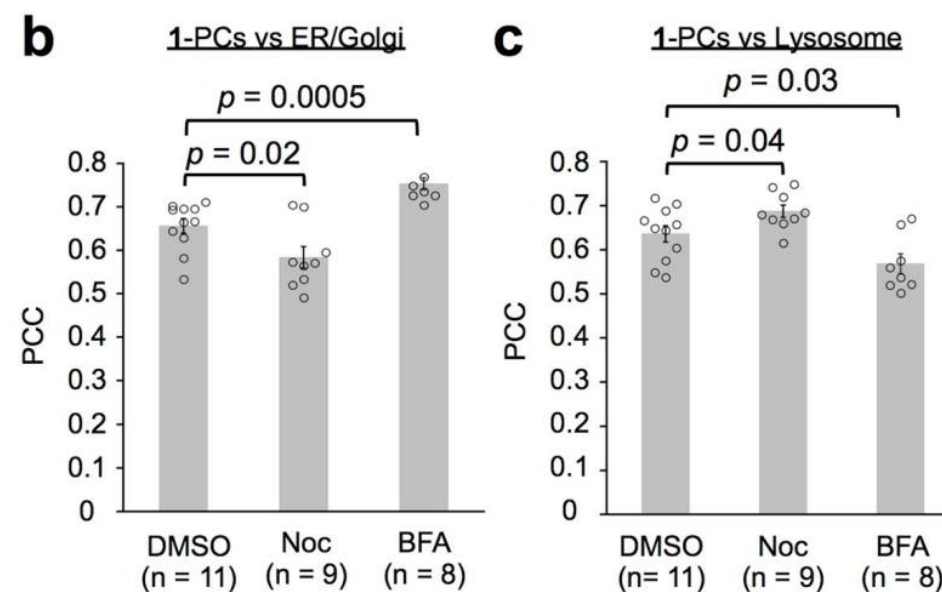
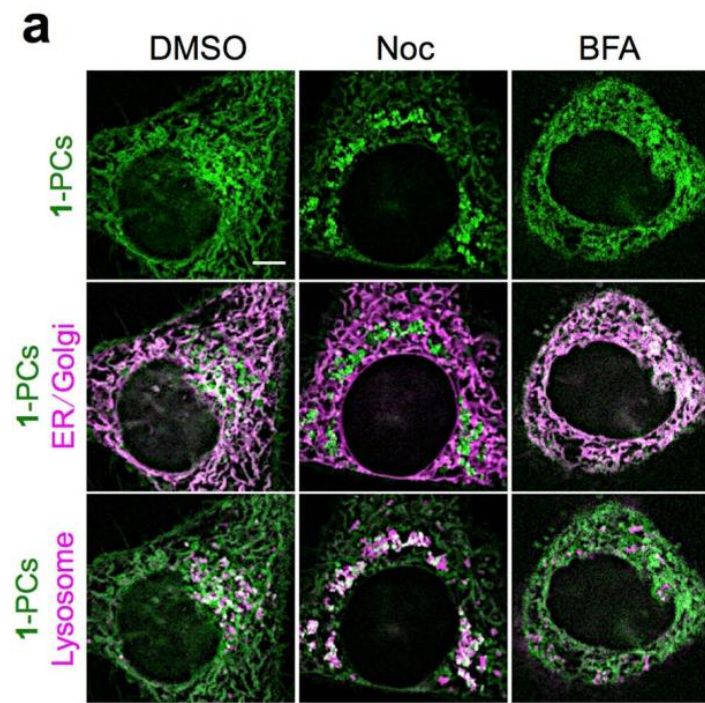


Extended Data Fig. 7 | Translocation of 2-PCs from mitochondria to lysosomes.





Extended Data Fig. 8 | Effects of Noc and BFA on interorganelle lipid transport



Extended Data Fig. 9 | Interorganelle lipid transport is affected by treatment of nocodazole (Noc) and brefeldin A (BFA)